International Journal of Applied Power Engineering (IJAPE)
Vol. 15, No. 2, June 2026, pp. 858~879
ISSN: 2252-8792, DOI: 10.11591/ijape.v15.i2.pp858-879

Rule-based energy management strategies for a hybrid microgrid using grey wolf optimizer

Sarmid Shakir Abdulsattar[1,2], Chee Wei Tan[1], Shahrin Ayob[1], Yasir Shakir Abdulsattar[3], Ahmed Tijjani Dahiru[4], Chin Kim Gan[5], Kwan Yiew Lau[1]
[1]Faculty of Electrical Engineering, Universiti Teknologi Malaysia, Johor, Malaysia
[2]Scientific Research Commission, Baghdad, Iraq
[3]Department of Mechanical Engineering, Faculty of Mechanical Engineering, Karabuk University, Karabuk, Turkiye
[4]Department of Electrical Electronics Technology, Federal College of Education (Technical), Bichi, Nigeria
[5]Department of Electrical Engineering, Universiti Teknikal Malaysia Melaka, Melaka, Malaysia

Article Info

Article history:

Received Nov 19, 2025
Revised Jan 26, 2026
Accepted Mar 12, 2026

Keywords:

Energy management system
Grey wolf optimizer
Levelized cost of energy
Microgrid
Optimization techniques
Renewable energy sources

ABSTRACT

This study utilizes grid-connected microgrids using photovoltaics (PVs) and wind turbines (WTs) in a residential system. For improved reliability, the system uses battery storage and diesel generators (Dgen). The proposed system uses supervisory controllers (as a rule-based energy management system) for energy management strategy implementations. The essence of using the grey wolf optimizer (GWO) is to strategize the rule-based energy management system in the proposed microgrid operations. The primary objectives are to achieve a low levelized cost of energy (LCOE) and determine the optimal number of microgrid components. The performance of the GWO is compared with three other optimization algorithms, namely, antlion optimizer (ALO), particle swarm optimizer (PSO), and cuckoo search algorithm (CSA), for benchmarking purposes. The findings indicate that the proposed GWO supersedes ALO, PSO, and CSO in energy cost reduction by 30.3% (0.0448 $/kWh), 65.6% (0.0971 $/kWh), and 120% (0.1774 $/kWh), respectively. The suggested algorithm selects the optimum number of the system's components, which is 46 PV modules, 30 wind turbines, and 10 units of batteries. An improved GWO-based algorithm based on hybridization with gradient descent algorithms is envisaged to implement a customer-centered energy management that can ensure customer satisfaction and further reduce energy cost.

Corresponding Author:

Chee Wei Tan
Faculty of Electrical Engineering, Universiti Teknologi Malaysia
Johor Bahru, 81310, Johor, Malaysia
Email: cheewei@utm.my

1. INTRODUCTION

Over the last century, the main contributor to climate change has been high carbon emissions. The combustion of fossil fuels produces between 70% and 75% of carbon emissions worldwide. The foregoing is considered to be the main contributor to the increasing global warming. Hence, mitigation of global warming has become one of the major environmental challenges of the present time due to the high increase in carbon emissions recorded annually [1]. Interest in harnessing renewable energy sources (solar and wind energy) has grown as a result of the decline in the use of fossil fuels, which includes the exhaustion of fossil fuel supplies, transportation of fuel, high operational costs, and fuel price fluctuations. Furthermore, the rate of increase in climate change affects renewable energy supplies. The foregoing factors motivated an investigation into hybrid energy systems to reduce environmental damage and harness the inexhaustible

renewable energy resources [2], [3]. Furthermore, these renewable energy sources (RESs) provide greater viability and ecological sustainability, presenting an alternative option to traditional energy systems. The implementation of renewable energy (RE) systems may promote economic growth, provide job opportunities, and improve general human well-being [4]. However, the unpredictable nature of these RESs necessitates the use of a storage device as a backup. To ensure the successful integration of RESs and energy storage systems (ESS) in microgrids, a meticulously designed and synchronized energy management scheme (EMS) is crucial to prevent extraneous expenses.

The fundamental concepts of microgrids as multi-energy systems have been elucidated in the literature. Multiple studies have investigated the effective control, capacity, and performance of hybrid renewable energy systems that include battery storage units. The scholar in [5] presented a rule-based algorithm and a metaheuristic optimization method known as the Levy flight algorithm (LFA) for the EMS of an autonomous hybrid renewable energy system, which employs a hydrogen and battery units as a storage system. The study in [6] proposed a hybrid system integrated with a utility grid. They used the ALO technique for sizing the components of the system using a rule-based energy management strategy to control the flow of power in the proposed microgrid. It is proposed in [7] that a standalone microgrid was integrated with renewable energy, diesel generators, and battery storage with environmental considerations to produce a new model for charging stations and employed the Giza pyramids construction algorithm (GPCA) for levelized cost of energy reduction. Adar *et al.* [8] created an independent photovoltaic energy generation system utilizing a multi-level DC–DC boost converter integrated with an artificial neural network-based maximum power point tracking technique to optimize power extraction under fluctuating irradiance and load conditions. The proposed method produced better voltage gain, quicker MPPT tracking, and less current ripple. However, grid-tied operation was not taken into account; instead, the study concentrated on PV performance at the component level. Due to the substantial expense of the microgrid, selecting a superior metaheuristic algorithm is essential. A little enhancement in the metaheuristic algorithms may significantly impact the estimated optimum capacity of the subsystems. Table 1 (see Appendix) demonstrates the critical analysis of the literature's optimization techniques, objectives, key findings, and limitations related to the microgrid system [9]-[16].

This study focuses on the integrated formulation by merging a rule-based energy management system with novel conditional renewable energy scenarios, which demonstrate unique priorities, control strategies, and optimization framework employed for the proposed grid-connected microgrid. Systematically comparing four sophisticated metaheuristic algorithms under uniform datasets and energy management restrictions, producing thorough analytical insights. In contrast, the previous studies often emphasize either system sizing or operational control independently. The following is a brief outline that delineates the main contributions of this study.

- The sizing approach of the proposed microgrid relies on a grid-connected photovoltaic/wind turbine/battery/diesel generator configuration, which emulates real microgrid performance. When PV and WT generate more energy than is required, the surplus energy will be sold to the grid; however, if surplus energy cannot fulfil the demands, the battery bank and diesel generator will supply the demands. If the energy produced from diesel and battery is not available, the proposed system will buy energy from the grid to meet the demands.
- A set of rule-based meta-heuristic algorithms has been implemented for creating a microgrid energy-control strategy and extracting concepts through the simulation system shown in Figure 1. It indicates that this particular EMS manages the flow and distribution of energy among the various microgrid components.
- A benchmark analysis is conducted among four algorithms to find the best optimal configuration of microgrid components, improve the use of renewable resources, and obtaining minimum value of LCOE.
- The study's findings show that the proposed system has improved the use of renewable resources, obtained an optimal system configuration, and reduced the LCOE.

In this research, a proposed five-step methodology for the design and optimization of a microgrid is introduced. The methodology involves the metrological data set, customer demand profiles, technical specifications of system components, and economic information. Figure 2 indicates the execution flow of the proposed system. The conceptual framework indicates how the sequence is arranged in phases, starting with data collection, proceeding through microgrid system configuration, energy management formulation, system sizing, simulation, result compilation, and analysis. Figure 2 illustrates the systematic representation of the research methodology used in the study to achieve the objective functions (minimizing LCOE, enhancing the utilization of renewable resources, and obtaining the optimal number of system components).

The rest of the paper is arranged as follows: Section 2 presents the case study as an overview with the aim of highlighting geographical location and the underlying weather parameters. Section 3 discusses the data collection approach (load demand and climatological data) of the proposed system in the research zone. Section 4 demonstrates the configuration and control framework of the grid-connected microgrid of the proposed system design. Section 5 introduces the mathematical modeling formulas for a grid-connected

microgrid employing diesel generators (Dgen) and energy storage system in conjunction with renewable energy systems. Section 6 studies and employs a supervisory control algorithm utilizing rule-based energy management strategies for managing power flow. Section 7 discusses the main objective functions with its constraint. Section 8 describes the implementation of the proposed algorithm (GWO) through descriptions and formulation, including benchmarking and optimization controlling parameters among four algorithms. Section 9 presents and discusses the findings of the proposed algorithm (GWO) with its counterparts (ALO, PSO, and CSA). Section 10 presents the technical justification of choosing GWO in the proposed microgrid. Finally, section 11, as a conclusive part of the paper, summarizes the research direction, procedure, and findings.

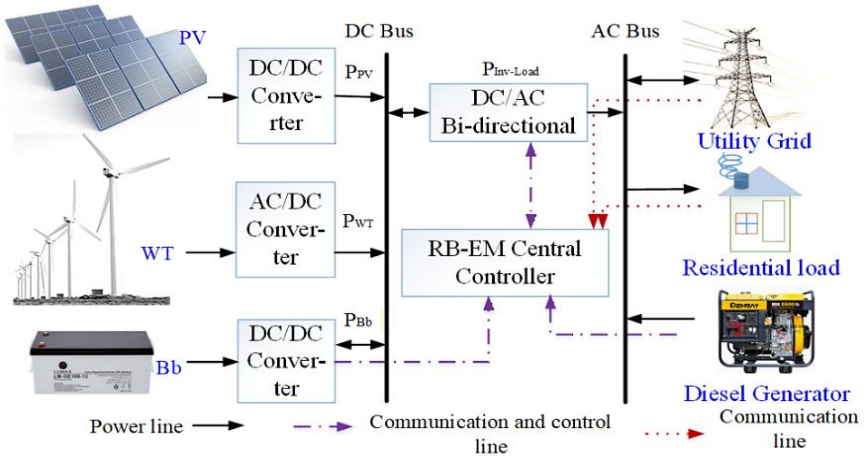

Figure 1. The architecture of the proposed microgrid for the research area

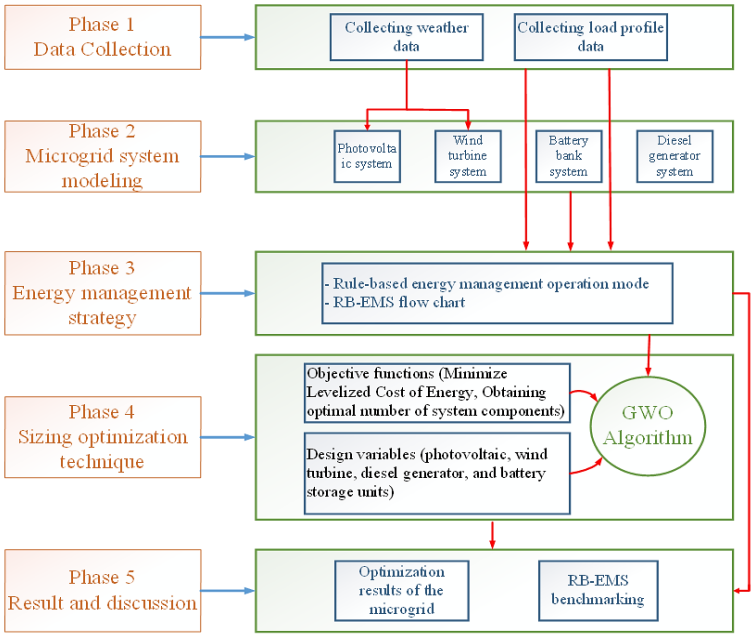

Figure 2. A systematic overview of system modeling for achieving the study objectives

2. CASE STUDY

This study focuses on the capital city of Iraq (Baghdad), situated centrally at a latitude of 33.3152° N and a longitude of 44.3661° E. This country is located in the MENA region (Middle East and North Africa). The daily average global solar irradiation in Iraq demonstrates remarkable geographical variation. The maximum value is shown in the desert areas and western surface, while the central and southern parts exhibit values between 4750 and 5000 Wh/m²/day. Studies indicate that Baghdad receives approximately

3,000 hours of solar irradiation each year. The monthly average wind speeds are 4.3 m/s in Baghdad, 4.3 m/s in Kerbela, 3.8 m/s in Tikrit, 2.8 m/s in Diwaniya, and 2.4 m/s in Kirkuk, as recorded by meteorologists. Additionally, the direct normal irradiance at the research site has varied between 5.4 and 5.5 kWh/m² [17], [18].

The geographical location of this study is characterized by four different seasons: winter, spring, summer, and autumn. The hourly data for an individual year have been collected, which include the ambient temperature (ranging from 8 to 51 °C), wind speed (varying from 1 to 10 m/s), solar irradiance (ranging from 5.1 to 7 kWh/m²/day), and load demand (varying from 2 to 7 kW/day). The data was acquired from the Renewable Energy Research Centre (RERC) in Iraq. This study combined solar and wind energy sources to meet the load demand. The storage battery banks have been used to address cloudy days, such as overcast or unfavorable weather. Further more thorough comprehension of consumer load requirements for various renewable energy sources has been attained via data analysis.

3. DATA COLLECTION

Iraq has an abundance of renewable energy sources, mostly solar and wind energy. The microgrid is evaluated for ten residential houses connected to the utility grid in Baghdad, Iraq. This study utilizes the load demand and climatological data in the specific equations to determine the generated power that is produced for the whole year. The proposed system has been modelled using actual metrological data. These data are recorded every single hour for the entire year (01/01/2023 to 31/12/2023). In addition, these data were collected from a ground-based meteorological station (Davis Instruments Vantage Pro 2), which was installed at the Ministry of Science and Technology (coordinates at 33.277193 latitude and 44.388113 longitude). It has a pyranometer, an anemometer, and a thermometer to measure the solar irradiance, wind speed, and ambient temperature, respectively. Figures 3, 4, and 5 illustrate the graphical representation of hourly data of wind speed, solar irradiance, and ambient temperature, respectively.

Energy demand has been collected and hourly recorded from local meters (installed by the Ministry of Electricity) in the residential house. The preprocessing steps used linear interpolation to impute missing data points. The processed data were classified into seasonal load variation in 2023 for the study area. Table 2 includes the average daily load, energy demand, and maximum daily load for each season. The load profile of the research region is predicated on seasonal fluctuations: summer (June, July, August), autumn (September, October, November), winter (December, January, February), and spring (March, April, May). Figure 6 depicts the load demand of all seasons. Data analysis is essential for a comprehensive knowledge of user load needs from various renewable energy sources. Summer demonstrates the peak load demand across all seasons and displays the greatest sensitivity to hourly fluctuations. In the early mornings (1:00 am–5:00 am), observe a decline in load demand, which reaches a low around 4:00 am due to a reduction in ambient temperature, thereby reducing the need for continuous cooling loads. The demand rises dramatically between 6:00 am and 8:00 am when appliances and cooling systems come online due to customers' needs. A relative decrease in demand starting at 9:00 am to 1:00 pm due to thermal energy storage and switching off the cooling systems (customers joining their work and left houses). During the late afternoon (2:00 pm), a comparatively high and continuously increasing demand is noticeable, indicating peak demand at 9:00 pm due to the increase in the ambient temperature, turning on the appliances, and continuous cooling loads. After 10:00 pm, the demand gradually decreases due to the switching off the appliances, except the cooling systems.

The demand levels in the winter load profile are moderate to high and clearly vary throughout the day. The fluctuation of demands follows approximately the same variance in summer with lower demands. Spring and autumn have the smoothest weather variance due to the stable climate change, thereby resulting in the lowest load demand. During these two seasons, the fluctuation of demand profile exhibits the same variance in Winter due to utilizing to the heating systems. While in autumn the demand reduces to a minimum level, such as at 1:00 am and at 11:00 a due to the elimination of the need for cooling devices.

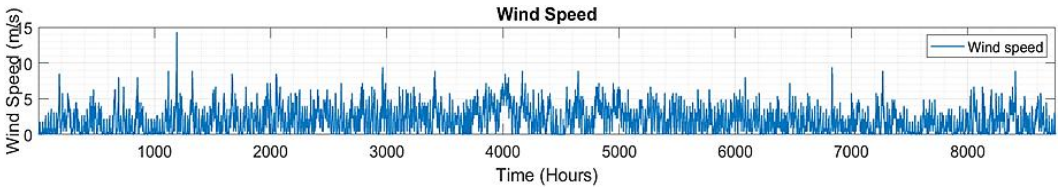

Figure 3. Annual data for wind speed in Baghdad/Iraq

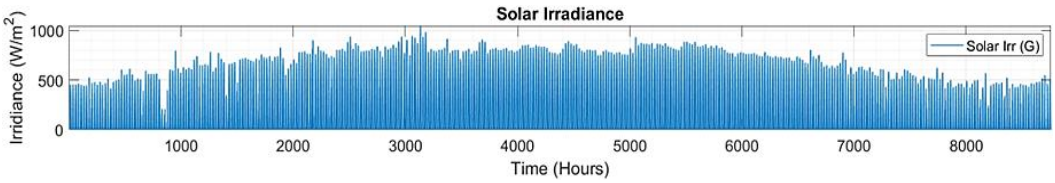

Figure 4. Annual data for solar irradiance in Baghdad/Iraq

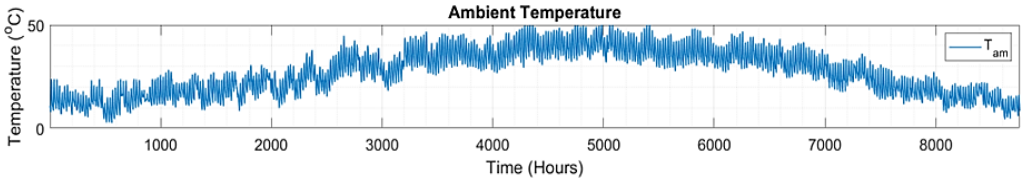

Figure 5. Annual data for ambient temperature in Baghdad/Iraq

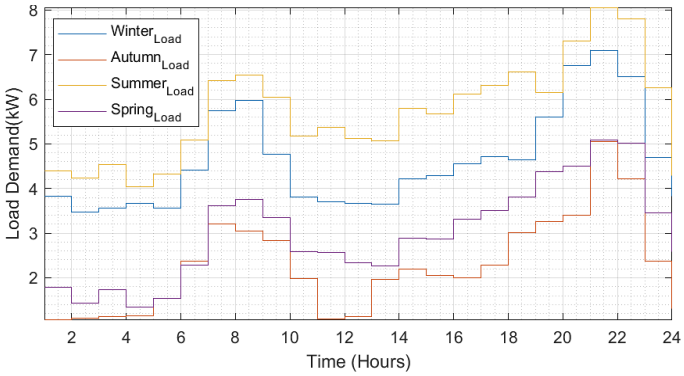

Figure 6. Daily load profile for a residential house in Baghdad, Iraq

Table 2. Seasonal load variation for the individual year (2023) in Baghdad/Iraq

Seasons	Average daily load (kW)/season	Maximum daily load/season(kW)	Seasonal energy demands (MWh)
Winter	95.7	121.17	206.71
Spring	68.26	90.98	150.72
Summer	107.70	142.51	237.81
Autumn	77.33	101.62	168.89

4. DESIGN OF THE PROPOSED MICROGRID

Numerous studies focus on microgrid operation scheduling, planning, and optimization. The hybrid proposed system shown in Figure 1 comprises renewable energy systems (photovoltaic and wind turbines), battery storage, diesel generators, and the AC residential load connected to the utility grid. This figure depicts the configuration and control framework of the grid-connected microgrid designed to meet the load demands of residential units. An AC-to-DC inverter links a wind turbine, while the photovoltaic array is connected via a DC-to-DC converter. Furthermore, the battery bank is linked via a bilateral DC-to-DC converter to facilitate the bidirectional conversion of power between AC and DC. The centralized controller and charger collaborate to coordinate the power flow to and from the battery bank. Moreover, it regulates the available energy among the integrated system components by utilizing an EMS [19], [20].

5. MODELING AND PARAMETERS OF THE PROPOSED MICROGRID

The physical and control architecture of the proposed system is designed to meet the demand of the residential loads in Iraq, as indicated in Figure 1. Modeling is the process of determining objectives, variables, and limitations associated with particular scenarios. Numerous papers have documented mathematical modeling formulas for a grid-connected system employing Dgen in conjunction with renewable energy resources. The modeled formulas of the RESs are extensively used by researchers to include all system components [21], [22].

5.1. Photovoltaic system

Various simulation models have been proposed in the literature [22]-[25] to compute the output power of solar systems. To determine the predicted output power of the PV system, the model must use the manufacturer's parameters together (see Table 3) with time-series data on solar irradiation and ambient temperature [26]-[30]. The model equation is presented in [24], [25], [31] and shown in (1) to ascertain the anticipated output power from the PV system.

$$P_{pv\_out} = P_{pv\_rated} \times \frac{G_t(t)}{1000} \times [1 + \alpha_t(T_C - T_{C\_STC})] \quad (1)$$

Where P_{pv_out} represents the output power of the photovoltaic module measured in watts (W); P_{pv_rated} is the rated power of the photovoltaic module under standard test conditions (STC) measured in watts (W); $G_t(t)$ represents the hourly solar irradiance data measured in watts per square meter (W/m²); α_t specify the temperature coefficient of the solar module, which is −3.6×10−3 (1/C°); and T_{C_STC} represents the cell temperature under standard test conditions, typically established at 25 °C. T_C denotes the cell temperature in degrees Celsius (°C), calculable by (2) [24]-[26], [31], [32].

$$T_C = T_{amb} + G_t \times \frac{T_{NOCT}-20}{800} \quad (2)$$

T_{amb} denotes the ambient temperature in degrees Celsius (°C), derived from time-series data, T_{NOCT} denotes the nominal operating cell temperature in degrees Celsius (°C), and PV manufacturers specify the T_{NOCT} value. The total power produced by photovoltaic panels (P_{pv_total}) in watt is determined by multiplying the output power of the photovoltaic module (P_{pv_out}) by the total number of photovoltaic modules in the system (N_{pv}) as depicted in (3) [25], [26].

$$P_{pv\_total} = N_{pv} \times P_{pv\_out} \quad (3)$$

Table 3. Economic and technical specifications of solar photovoltaic system

Components	Specifications	Values	Units
Solar photovoltaic [26]-[30]	Solar-rated power at STC	0.5	kW
	Temperature coefficient	-0.36	%/ºC
	Nominal operating cell temperature	41± 3	ºC
	Efficiency	20.9	%
	Lifetime	20	Years
	Investment cost	600	$/unit
	Replacement cost	350	$/unit
	Operation and maintenance cost	6	$/kWh/year

5.2. Wind power system

The second renewable energy generator is the wind turbine, which is the most often used globally. It can harness the maximum amount of wind energy available during day hours and transform it into electrical power. Wind turbines are classified into two categories: vertical-axis turbines and horizontal-axis turbines. The horizontal-axis design is predominant among contemporary commercial wind turbines, whereby the blades spin parallel to the wind flow. The advantages of these turbines are increased efficiency, reduced cut-in wind speeds, and lower costs per kWh of output. The (4) has been used for determining the output power generated from turbines [26], [33], [34] by utilizing the technical specification of wind turbines in Table 4.

$$P_{WT_{out}} = \begin{cases} 0 & v(t) \le v_{cut-in} \quad or \quad v(t) \ge v_{cut-out} \\ P_{WT_{rated}} \times \dfrac{v(t) - v_{cut-in}}{v_{rated} - v_{cut-out}} & v_{cut-in} < v(t) < v_{rated} \\ P_{WT_{rated}} & v_{rated} < v(t) < v_{cut-out} \end{cases} \quad (4)$$

$P_{WT_{out}}$ represents the output power generated by a wind turbine in kW and $P_{WT_{rated}}$ denotes the rated output power in watts (W). Furthermore, v_{rated} denotes the rated wind speed in m/s, v_{cut-in} signifies the low cut-in speed in m/s, whereas $v_{cut-out}$ indicates the high cut-out speed in m/s, $v(t)$ depicts the wind speed at turbine hub height in m/s. The total output power generated by wind turbines ($P_{TWT_{out}}$) in kW can be calculated by multiplying $P_{WT_{out}}$ with the total number of installed wind turbines (N_{WT}) as illustrated by the following (5) [26], [33], [34].

$$P_{TWT_{out}} = P_{WT_{out}} \times N_{WT} \quad (5)$$

As shown in (6), the generated power from wind turbines may be computed more accurately by taking hub height (h) into account [34]. Here, h is defined as the correlation between altitude and wind velocity in m. v denotes the rated velocity of the wind turbine in m/s, while v_{ref} is the speed of wind flow in (m/s). An anemometer measures them at a reference height of h_{ref} in m, while the hub height is indicated by h. Furthermore, the landscape friction coefficient is denoted by $\gamma*$. This coefficient (γ*) varies among locations based on the topological surface of that region, which is used as 0.1 in a flat field and 0.25 in a non-flat field. Figure 7 illustrates the power characteristics curve of the wind turbine.

$$v = v_{ref} \times (h/h_{ref})^{\gamma*} \quad (6)$$

Table 4. Economic and technical specifications for wind turbines

Components	Specifications	Values	Units
Wind turbine [27], [28], [35], [36]	Turbine rated power	1	kW
	Cut-in speed ($Vcut-in$)	2	m/s
	Cut-out speed ($Vcut-out$)	40	m/s
	Rate Speed (Vr)	9	m/s
	Blades diameter	2.4	m
	Lifetime	20	Years
	Investment cost	2300	$/unit
	Replacement cost	1500	$/unit
	Operation and maintenance cost	23	$/kWh/year

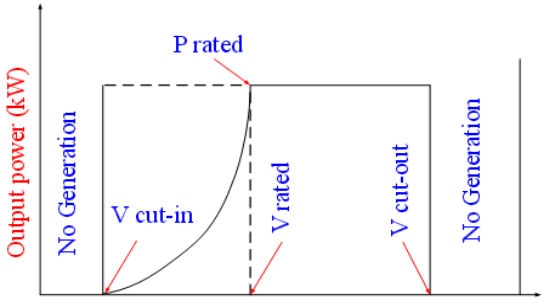

Figure 7. The operational region of the ideal power curve and wind speed [33], [34]

5.3. Battery energy storage system

The energy produced by RERs (solar and wind energy) that is not always accessible has to be stored in a battery bank. It is utilized as backup energy that supplies homes on cloudy days. In (7) is used to determine the battery storage capacity in ampere-hours (Ah) [6] by depending on the technical specifications in Table 5. Here, C_{bat} represents the rated capacity of the rechargeable battery in Ah, and D_{auto} denotes the duration of days devoid of solar irradiance (autonomy days, which is 3-5 days). E_{load} denotes the mean daily load required in kW, V_{sys} is the system operating voltage (48 volts), DoD indicates the maximum permissible depth of discharge for the battery (80%) as indicated in Figure 8, and η_{inv}, η_{batt} indicate an inverter and battery efficiency of 95%, 85%, respectively.

$$C_{bat} = \frac{E_{load} \times D_{\text{auto}}}{\eta_{batt} \times \eta_{inv} \times DoD \times V_{sys}} \quad (7)$$

Table 5. Economic and technical specifications for battery bank

Components	Specifications	Values	Units
Battery storage bank [24], [27], [28], [36]	Battery nominal voltage	12	V
	Nominal capacity	40	Ah
	Lifetime	5	Years
	Efficiency	85	%
	Initial SoC of battery	100	%
	SoCmin	20	%
	SoCmax	100	%
	Depth of discharge (DoD)	0.8	%
	Initial capital cost	176	$/unit
	Replacement cost	67	$/unit
	Operation and maintenance cost	5.28	$/kWh/year

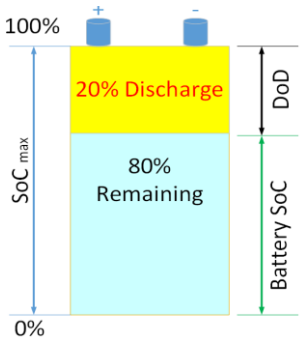

Figure 8. The principal concept of DoD and SoC in the storage battery

5.4. Diesel generation specifications

The major focus for the microgrid backup supply is the battery bank, which functions as the main backup, while the diesel generators (Dgen) is a secondary backup supplier. Power generation depends on the availability of renewable energy resources (solar and wind energy). In the absence of these resources, and the battery bank attains the minimum state of charge (SoC), the Dgen would commence operating to meet customer demands. The subsequent (8) are employed to model the Dgen with its fuel consumption [27], [28], [37] by using the technical specifications in Table 6 and Table 7.

$$F_{con}(t) = A_g P_{Dgen}(t) + B_g P_{Dgenr}(t) \quad (8)$$

Where $F_{con}(t)$ represents fuel consumption measured in Liter/h, A_g represents the coefficient of fuel consumption (0.24 Liter/kWh), P_{Dgen} (t) denotes the output power from the diesel generator in (kW), B_g is an additional coefficient of fuel consumption (0.084 Liter/kWh), and $P_{genr}(t)$ denotes the generator's rated power in kW. The fuel cost (F_{cost}) in US$/h throughout the system's lifetime is delineated in (9) [32], [38].

$$F_{cost} = (C_{price} \sum F_{con}(t)) \times C_{pv} \quad (9)$$

C_{price} represents the present cost of diesel fuel for each liter (US$/Liter) and C_{pv} represents the cumulative present value throughout a temporal spectrum; its calculation may be found in (10) [32].

$$C_{pv} = R_i (1 + R_i)^T / (1 + R_i)^T - 1 \quad (10)$$

Where R_i denotes the interest rate and T denotes the project's life time (20 years).

Table 6. Economic and technical specifications for diesel generator

Components	Specifications	Values	Units
Diesel generator [27], [30], [36]	Rated power of the diesel generator	4	kW
	Initial cost	700	$/unit
	Lifetime	20,000	hours
	Lifetime	9	years
	Replacement cost	700	$/unit
	Operation and maintenance cost	8	$/kWh/year
	Fuel cost	1	$/liter

Table 7. Economic parameters of the proposed system

Components	Specifications	Values	Units
Economic parameters [37]-[39]	Lifespan of the project	20	Years
	Inflation rate	2	%
	Interest rate	6	%

5.5. Power converter

Bi-directional inverter connects between the AC and DC bus, which transfers the power from the energy sources to the loads. It is modeled based on its efficiency. It is essential to note that any selected converter must be capable of handling the maximum anticipated AC loads and the potential surges that occur

during the first startup of gadgets. The inverter rating $P_{inv}(t)$ in kW may be determined using (11) [32], [40] and Table 8.

$$P_{inv}(t) = \frac{P_L^m}{\eta_{inv}} \quad (11)$$

Where the P_L^m indicates the peak residential load demand in kW, which is considered the crucial factor in selecting the appropriate inverter, and the inverter efficiency is represented by η_{inv}.

5.6. Utility grid integrations

The primary grid can provide electricity to the microgrid in the absence of a renewable energy sources, Dgen, and at a minimum SoC(t). Table 9 [41] and (12) are used to calculate the income (I_{grid}) in US$ from the energy generated by photovoltaic systems (PV) and wind turbines (WT) to the utility grid [42].

$$I_{grid} = \sum_{t=1}^{8760} R_{feed\ in\ tariff} \times E_{grid-sell} \quad (12)$$

Where $R_{feed\ in\ tariff}$ pertains to the feed-in tariff rate expressed in $/kWh, $E_{grid-sell}$ refers to the energy sold to the utility grid in kWh, and the total number of hours in a year is represented by 8760. Furthermore, (13) is used to calculate the price of purchasing energy acquired (C_{Grid}) in US$ from the grid [36].

$$C_{Grid} = C_b \times \sum_{t=1}^{8760} E_{grid-purchased} \quad (13)$$

Where C_b denotes the cost of acquiring 1 kW of electricity from the grid in $/kWh [37], $\sum_{t=1}^{8760} E_{grid-purchased}$ refers to the total energy purchased from the utility grid for the individual year in kWh.

Table 8. Economic and technical specifications for inverter

Components	Specifications	Values	Units
Inverter [7], [27], [28]	Inverter capacity	1	kW
	Efficiency	95	%
	Lifespan	15	Years
	Capital cost	127	$/unit
	Replacement cost	127	$/unit
	Operation and maintenance cost	1	$/kWh/year

Table 9. Economic specifications for utility grid

Components	Specifications	Values	Units
Utility Grid [41]	Purchase price	0.023	$/kWh
	Selling price	0.015	$/kWh

6. SUPERVISORY CONTROL ALGORITHM

This study employs a supervisory control algorithm for managing power flow. There are three primary categories of these algorithms: learning-based (LB), rule-based (RB), and optimization-based (OB). Each algorithm works independently and produces differing levels of precision in its findings. The rule-based energy management strategies have been particularly selected for the investigation in concern.

6.1. The proposed rule-based energy management strategies

The most important criterion in microgrid design is a resilient energy management system (EMS). The RB-EMS has been proposed to regulate the power distribution among different parts of the microgrid [43]. RB-EMS additionally enhances system efficiency, reduces battery deterioration, optimizes the use of renewable energy sources, and decreases fuel consumption, yielding considerable cost advantages and energy conservation. Furthermore, they provide real-time control with minimum computational requirements [44]. This article examines six operational scenarios for the best functioning of grid-connected microgrids. These scenarios adhere to a certain set of predetermined instructions. Table 10 presents the RB-EMS scenarios for the proposed microgrid situations.

6.2. Sequential flow of the rule-based energy management strategy

The unpredictable nature of renewable energy supplies and the irregularity of demand are the primary factors that complicate the EMS. Consequently, fulfilling energy demand with a single energy source is unfeasible economically and technically due to constraints in availability, dependability, and scalability. To maintain the balance between power generation and demand, a diesel generator and storage battery units may

be integrated with renewable energy sources. Nonetheless, the proposed system must ensure the complete use of renewable energy sources while minimizing the usage of the diesel generator and storage battery. This is achievable just with a suitable and well-crafted RB-EMS approach. The primary objective of the EM method is to coordinate and efficiently manage the energy composition of the microgrid components [45]. The proposed EMS comprises RB frameworks, mostly using "if" and "then" statements. The flowcharts of RB EMS are demonstrated in Figure 9, which shows the priority operation steps of system components to meet the load demand [46].

Table 10. Operational scenarios of the proposed microgrid

Scenarios	Operation scenarios
Mode 1	The generated energy from the RE systems (WT and PV) supplies the residential loads with electric power.
Mode 2	The excess energy generated by the RE systems (WT and PV) covers the load demands, and charges batteries if SoC(t)<SoC(t) max.
Mode 3	Energy generated by the RE systems (WT and PV) exceeds the load demands, and the battery's status is SoC(t)=SoC(t)max, then the surplus energy will be sold to the utility grid (sell to the grid).
Mode 4	If the energy generated by the RE systems (WT and PV) is not enough to fulfill the load demand, and the batteries' status is SoC(t)>SoC(t)min, then the stored energy in the battery bank will be utilized to feed the load demands.
Mode 5	Energy generated by the RE systems (WT and PV) is not enough to fulfil the load demand, and the battery's status is SoC(t)<SoC(t)min, then the diesel generator (Dgen) will be utilized to feed the load demands and charge the battery bank.
Mode 6	Energy generated by the RE systems (WT and PV) is not enough to fulfil the load demand, and the battery status is SoC(t)<SoC(t)min. In addition, the Dgen does not work or does not cover the demands; in this regard, the utility grid will be utilized to feed the load demands and charge the battery bank (purchased from the utility grid).

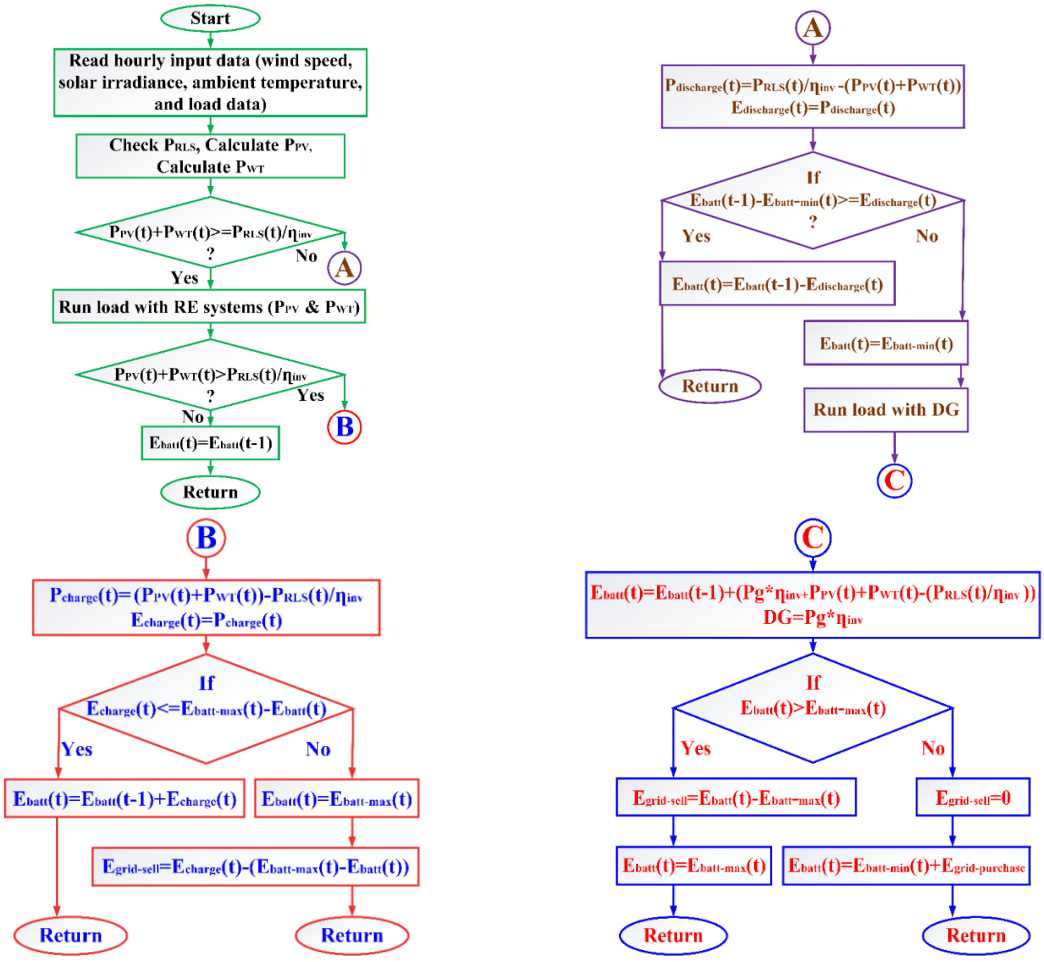

Figure 9. Flowcharts of the sequential flow of the rule-based energy management strategies

Figure 9 is divided into four flowcharts; the main flowchart (it generates A and B flowcharts) depicts the first decision, which runs hourly. It begins by reading the metrological data set. Then find the output power from photovoltaic (PPV) and wind turbine (PWT) systems. After that, the RB-EMS will do the

first comparison regarding the energy produced from renewable energy resources, whether it is equal to load demands or not ($P_{PV}(t)+P_{WT}(t)>=P_{RLS}(t)/\eta_{inv}$). If it is equal, then the energy produced will supply the demands; if not, go to flowchart A. The second comparison will check energy produced from renewable energy resources, whether it is bigger than demands or not ($P_{PV}(t)+P_{WT}(t)>P_{RLS}(t)/\eta_{inv}$). If it is bigger, go to flowchart B; if it is not, obtain energy from the storage bank.

In flowchart A, the RB-EMS calculates the energy discharge from storage battery bank ($P_{discharge}(t)=P_{RLS}(t)/\eta_{inv}-(P_{PV}(t)+P_{WT}(t)$ and checking whether it covers the deficit in renewable energy or not ($E_{batt}(t-1)-E_{batt-min}(t)>=E_{discharge}(t)$) , if yes, then utilize the storage bank to meet the demands ($E_{batt}(t)=E_{batt}(t-1)-E_{discharge}(t)$), if not then D_{gen} will fulfill the demands ($E_{batt}(t)=E_{batt-min}$) thereby go to flowchart C. Flowchart C deals with D_{gen}, it demonstrates that the combination energy produced by renewable resources and D_{gen} will fully charge the battery bank and supply the demands ($E_{batt}(t)=E_{batt}(t-1)+(Pg*\eta_{inv}+P_{PV}(t)+P_{WT}(t)-(P_{RLS}(t)/\eta_{inv})$), then RB-EMS will check if $SoC(t)>SoC(t)_{max}$ ($E_{batt}(t)>E_{batt-max}(t)$) or not, if it is bigger, the surplus energy will be sell to the grid ($E_{grid-sell}=E_{batt}(t)-E_{batt-max}(t)$), if it is $SoC(t)<SoC(t)_{max}$, the RB-EMS will import from the utility grid (called grid purchase) ($E_{batt}(t)=_{Ebatt-min}(t)+E_{grid-purchase}$) to charge the battery and fulfill the demands.

While in flowchart B, RB-EMS will check whether surplus energy from renewables less than or equal the difference between $SoC(t)_{max}$ and SoC(t) ($E_{charge}(t)<=E_{batt-max}(t)-E_{batt}(t)$), if it is bigger ($E_{charge}$), then the excess energy will charge the battery to be $SoC(t)=SoC(t)_{max}$ ($E_{batt}(t)=E_{batt-max}(t)$) and sell the rest energy to the grid, if not, the excess energy will charge the battery ($E_{batt}(t)=E_{batt}(t-1)+E_{charge}(t)$).

7. OBJECTIVE FUNCTION FOR THE PROPOSED MICROGRID

The main objective of this research is to reduce the levelized cost of electricity (LCOE) of the proposed system while ensuring optimal energy flow and choosing the optimal number of the proposed system components. LCOE is a vital indicator for evaluating the economic competitiveness of various energy-generating technologies, such as conventional (diesel and gas power plants) and non-conventional (PV, WT, hydropower, and Biomass plants) generation systems. It is characterized as the ratio of yearly system cost (A_{SC}) in (\$/year) proportion to the total energy generated (P_g) of microgrid components in (kWh/year) over a specific period [47]. The mathematical modelling (14) is employed to calculate the LCOE in US\$/kWh [26], [48], [49].

$$LCOE = A_{SC}/P_g \tag{14}$$

The yearly system cost (A_{SC}) is a prominent metric used to assess the economic viability of a grid-connected microgrid [50]. The subsequent expression (15) delineates the procedure for computing A_{SC} [26].

$$A_{SC} = N_{PV}C_{Solar-PV} + N_{WT}C_{Wind\ Turbine} + N_{BT}C_{Battery-Bank} + N_{INV}C_{Inverter} + N_{DG}C_{Diesel\ Generator} + C_{Grid} - I_{grid} \tag{15}$$

Where N_{PV}, N_{WT}, N_{BT}, N_{INV}, N_{DG} demonstrate the total numbers of PV modules, wind turbines, batteries, inverters, and diesel generators, respectively. C_{Grid} shows the cost of buying energy from the grid (USD\$/kWh), and I_{grid} indicates the profits from selling energy to the grid (USD\$/kWh). Furthermore, to acquire the A_{SC}, the expenses of each system component must be computed individually, as shown in (16) to (20) [26], [30], [40].

Photovoltaic module: $C_{Solar-PV} = C_{PV-Invest} + C_{PV-Repla} + C_{PV-O\&M}$ (16)

Wind turbine: $C_{Wind\ Turbine} = C_{WT-Invest} + C_{WT-Repla} + C_{WT-O\&M}$ (17)

Battery unit: $C_{Battery-Bank} = C_{Batt-Invest} + C_{Batt-Repla} + C_{Batt-O\&M}$ (18)

Inverter: $C_{Inverter} = C_{Inv-Invest} + C_{Inv-Repla} + C_{Inv-O\&M}$ (19)

Diesel generator: $C_{Diesel\ Generator} = C_{Dgen-Invest} + C_{DG-Repla} + C_{Dgen-O\&M}$ (20)

Where $C_{Solar-PV}$, $C_{Wind\ Turbine}$, $C_{Inverter}$, $C_{Battery-Bank}$, and $C_{Diesel\ Generator}$ denote the cost of photovoltaic modules, wind turbines, inverters, battery bank, and diesel generators in (USD\$/unit), respectively. Furthermore, $C_{PV-Invest}$, $C_{WT-Invest}$, $C_{Batt-Invest}$, $C_{Inv-Invest}$, and $C_{Dgen-Invest}$ represent the installation costs of photovoltaic modules, wind turbines, batteries, inverters, and diesel generators in

(USD$/unit), respectively. While $C_{PV-Repla}$, $C_{WT-Repla}$, $C_{Batt-Repla}$, $C_{Inv-Repla}$, and $C_{Dgen-Repla}$ denote the replacement costs of solar panels, wind turbines, batteries, inverters, and diesel generators in (USD$/unit), respectively. The $C_{PV-O\&M}$, $C_{WT-O\&M}$, $C_{Batt-O\&M}$, $C_{Inv-O\&M}$, and $C_{DG-O\&M}$ represent the yearly operational and maintenance (O&M) costs of solar panels, wind turbines, batteries, inverters, and diesel generators in (USD$/kWh/year), respectively [30], [40].

The objective functions are constrained by the following limitations:

- Decision variables constraint

The aspects of choosing the upper and lower bounds for optimization variables depend on the problem structure (number of variables and search space). The constraint is illustrated in (21).

$$M_X^{min} \leq M_X \leq M_X^{max} \tag{21}$$

Where M_X is the number of the proposed system components, M_X^{min} demonstrates the minimum number of components, and M_X^{max} indicates the maximum number of components. The lower bound demonstrates by 10, 20, and 10 for wind, solar, and Battery, respectively. The upper bound is depicted by 30, 46, and 60 for wind, solar, and battery, respectively.

- Battery constraint

To increase battery longevity, the battery bank's state of charge (SOC) must remain steady between its highest state of charge (SoC_{max}) and lowest state of charge (SoC_{min}), ensuring that the battery storage bank is never completely charged or totally depleted during operation. The constraint is demonstrated in (22).

$$SoC_{min} \leq SoC(t) \leq SoC_{max} \tag{22}$$

8. METAHEURISTIC OPTIMIZATION TECHNIQUES

Optimization algorithms are considered the optimal selection of an alternative solution set for cost-effective or superior performance [51]. The proposed algorithm is classified as a nature-inspired metaheuristic optimization technique capable of addressing microgrid issues. Power flow issues may be addressed using many techniques, one of which is GWO. GWO has been used in the current study and compared with ant lion optimizer (ALO), cuckoo search algorithm (CSA), and particle swarm optimizer (PSO) as benchmark algorithms. The key measures for assessing the performance of an optimization strategy are time, accuracy, and optimality [52], [53]. GWO is primarily inspired by the hunting strategies and leadership behaviors of grey wolves. When mathematically articulated, the algorithm identified alpha wolf as the best appropriate option. The second and third ideal solutions are designated as beta and delta wolves. The remaining possible solutions are considered to be omega wolves. The wolf social hierarchy is depicted in Figure 10.

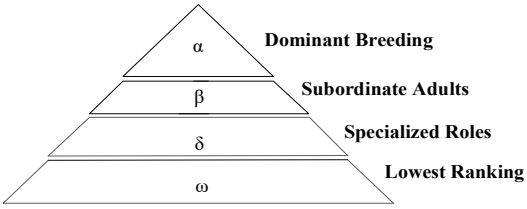

Figure 10. Diagram of the grey wolf social hierarchy [54]

Furthermore, it was suggested to use (23) and (24) for the encirclement of targets and the hunting of grey wolves.

$$\vec{D} = |\vec{C}.\overrightarrow{X_p}(t) - \vec{X}(t)| \tag{23}$$

$$\overrightarrow{X(t+1)} = \overrightarrow{X_p}(t) - \vec{A}.\vec{D} \tag{24}$$

Where $\overrightarrow{X_p}$ indicates the position of the prey vector, $\vec{X}$ represents the position vector of the gray wolf, whereas t indicates the current status of the iteration. The coefficient vectors $\vec{A}$ and $\vec{C}$ are calculated using the formulae specified in (25) and (26).

$$\vec{A} = 2\vec{a}.\overrightarrow{r_1} - \vec{a} \tag{25}$$

$$\vec{C} = 2.\overrightarrow{r_2} \quad (26)$$

Where the intermittent vectors ranging from 0 to 1 are represented by r_1 and r_2. Throughout the iteration, $\vec{a}$ is diminished from 2 to 0. Grey wolves use alpha leadership to identify and encircle their prey. Nonetheless, the optimal prey's position inside the search space remains unidentified. The alpha, beta, and delta mathematical models of grey wolf hunting activities can describe their activity. They imparted to the wolves enhanced awareness of the potential location of the prey. Consequently, as seen in (27) to (33), the three optimal solutions are preserved, but the remaining solutions (omegas) must be recalibrated to more advantageous positions [55], [56].

$$\overrightarrow{D_\alpha} = |\overrightarrow{C_1}.\overrightarrow{X_a} - \vec{X}| \quad (27)$$

$$\overrightarrow{D_\beta} = |\overrightarrow{C_2}.\overrightarrow{X_\beta} - \vec{X}| \quad (28)$$

$$\overrightarrow{D_\delta} = |\overrightarrow{C_3}.\overrightarrow{X_\delta} - \vec{X}| \quad (29)$$

$$\overrightarrow{X_1} = \overrightarrow{X_a} - \overrightarrow{A_1}.(\overrightarrow{D_a} \quad (30)$$

$$\overrightarrow{X_2} = \overrightarrow{X_\beta} - \overrightarrow{A_2}.(\overrightarrow{D_\beta}) \quad (31)$$

$$\overrightarrow{X_3} = \overrightarrow{X_\delta} - \overrightarrow{A_3}.(\overrightarrow{D_\delta} \quad (32)$$

$$\vec{X}(t+1) = \overrightarrow{X_1} + \overrightarrow{X_2} + \overrightarrow{X_3}\Big/_3 \quad (33)$$

Grey wolves stop hunting when their prey becomes immobile. This approach is mathematically described by reducing the value of $\vec{a}$ from 2 to 0. Consequently, A gets a drop, since the value of $\vec{A}$ is dependent on the value of $\vec{a}$. Wolves initiate attacks to catch prey when the values of $\vec{A}$ range from -1 to 1. GWO has a variable denoted as $\vec{C}$, which spans from 0 to 2. This variable adjusts the weights for prey to stochastically emphasize ($\vec{C}$> 1) or de-emphasize ($\vec{C}$< 1) their importance in determining the distance. This component is particularly beneficial in the last iteration for extricating the solution from local optima. A summary of the proposed GWO method for addressing the problem is provided in Table 11, while Table 12 demonstrates the controlling parameters among the four optimization techniques [56]-[58].

Table 11. Details of the proposed GWO algorithm for solving problems [55]-[58]

Steps	Procedures	Functions
Step 1	Load input data	Load the meteorological database (wind speed, solar radiation, and ambient temperature). Load a load demand database. Load the database containing the techno-economic parameters of the microgrid components as shown in Tables 3-9. Load the economic factors (project's lifetime and interest rate) (see Tables 3-9).
Step 2	Initialize algorithm parameters	GWO constants: Max. iterations =100, search agents = 2 Set the search space: The maximum and minimum limits for the PV quantity [46, 20]. The maximum and minimum limits for the WT quantity [30, 10]. The maximum and minimum limits for the Bat quantity [60, 10].
Step 3	Initialize the population of the grey wolf optimizer	Randomly produce an initial population of potential solutions inside the specified search space. Each solution demonstrates a combination of microgrid component dimensions (e.g., quantity of photovoltaic and wind turbines).
Step 4	Examine the fitness of each individual	Determine the three optimal solutions and designate them as α, β, and δ as first, second, and third best, respectively. Determine the objective function (LCOE) for each possible solution.
Step 5	Update the locations of all remaining wolves (ω)	Utilize the position updating equations of the grey wolf optimizer, predicated on the effect of the α, β, and δ wolves: $\vec{X}(t+1) = \overrightarrow{X_1} + \overrightarrow{X_2} + \overrightarrow{X_3}\Big/_3$
Step 6	Examine the new candidate solutions	Determine the fitness values of the revised population. Revise the locations of α, β, and δ if superior solutions are identified.
Step 7	Reiterate the position modification	Continue updating locations employing the GWO mechanism across all iterations, facilitating the algorithm's steady convergence to the ideal solution.
Step 8	Ending condition	Upon reaching the maximum iteration limit or fulfilling the convergence requirement, return the optimum configuration represented by the best solution (α wolf). If not, return to step 5.

Table 12. The benchmark and optimization controlling parameters among the fourth algorithms [55], [56], [59]-[61]

GWO technique	ALO technique	CSA technique	PSO technique
Population size = 2 Max. iteration = 100 Convergence reaches the highest number of iterations	Search agents = 2 Max. iteration = 100 Convergence is equal to the stability of the fitness value of elite antlions or reaches the highest number of iterations	Number of nets = 2 Max. iteration = 100 Convergence is equal to minimal modification to the global optimal solution	Population size = 2 Max. iteration =100 Convergence represents the minimum variation in the global best fitness value across a predetermined number of iterations
Leadership roles: α, β, and δ Lower bound wind, solar, and battery: 10, 20, 10 Upper bound wind, solar, and battery: 30, 46, 60 No. of leaders: 3 (α, β, and δ)	Best score: Elite antlion fitness Lower bound wind, solar, and Battery: 10, 20, 10 Upper bound wind, solar, and battery: 30, 46, 60 Selection method: Roulette wheel	Initial weight: 0.4 Lower bound wind, solar, and battery: 10, 20, 10 Upper bound wind, solar, and battery: 30, 46, 60 Levy flight: Used for step size	Initial weight: 0.4 Lower bound wind, solar, and battery: 10, 20, 10 Upper bound wind, solar, and battery: 30, 46, 60 Weighting factors (C1 and C2): 2

9. RESULTS AND DISCUSSION

The developed methodology employed in this study is based on a rule-based control system combined with optimization approaches, utilized to construct a compact hybrid system that comprises two primary renewable energy sources (wind and solar energy), which are integrated with a battery and with a diesel generator as a backup system, and connected to the grid. The technical and economic data of this study have been examined and used with specified optimization methods for benchmark purposes (see Tables 3 to 9). Figures 11(a) and 11(b) illustrate the output power generated by the solar PV system and wind turbine system, as determined by (1) and (4), respectively. The output power of the PV system is contingent upon the existing climatic conditions, particularly when considering ambient temperature (T_{amb}) and solar irradiance (G). The interpretation of low solar power production in the first 8 days of February 2023, as indicated in Figure 11(a), was due to cloudy and rainy days, thereby reducing the solar irradiance in the proposed study area during that time, which led to limited solar power generation. The output power of the wind generator is determined by the rated speed (v_{rated}), cut-out speed ($v_{cut-out}$), and cut-in speed (v_{cut-in}), as defined by the company that produces it. The power generation from wind turbines is almost non-existent in February and November 2023, as indicated in Figure 11(b), during which time this is attributed to a significant decrease in wind speed in the study area.

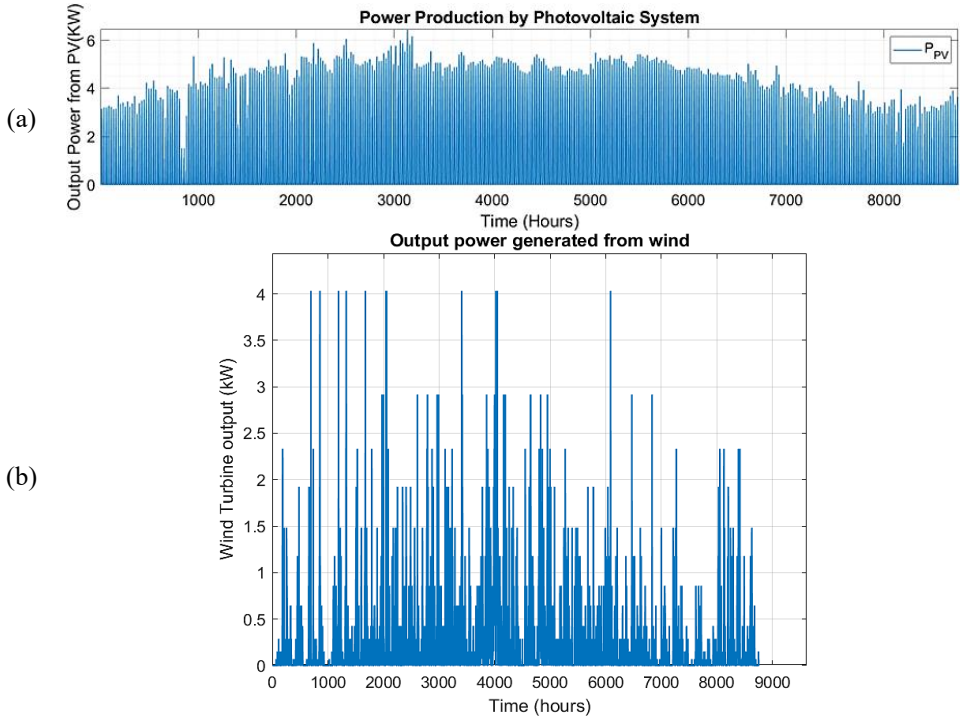

Figure 11. Annual output power of (a) the solar PV system and (b) the wind turbine system

Additionally, the optimal convergence is illustrated in Figure 12, which compares four optimization techniques, and the governing parameters are listed in Table 12. The first optimization technique (GWO) converged in around 3 iterations, the second (ALO) took approximately 16 iterations, the third (PSO) took approximately 5 iterations, and the fourth technique (CSA) took approximately 3 iterations. The results indicate that the LCOE in GWO is less than that of other algorithms, demonstrating that GWO achieves superior outcomes compared to other benchmark methods due to its faster and more stable convergence speed. Moreover, it achieves a superior equilibrium between exploration and exploitation via its hierarchical leadership. All simulations were implemented in MATLAB R2023b, which is executing at 1.80 GHz on an Intel Core i7 CPU. Table 13 shows the LCOE for the last iteration (100 iterations) of these techniques and the optimal number of microgrid components required to utilize RESs in the research area. The findings indicate that the proposed GWO supersedes ALO, PSO, and CSO in energy cost reduction of 30.3% (0.0448$/kWh), 65.6% (0.0971$/kWh), and 120% (0.1774$/kWh), respectively.

Furthermore, GWO chooses the optimal number for the proposed system; except for the capacity of the diesel generator, it has been assumed to be a constant capacity (1 kW). The last iteration demonstrates the ending comparison of LCOE among these techniques, which is presented in US$, as seen in Figure 13. Figure 14 illustrates the graphical representation findings for the annual system cost of microgrid components using the GWO technique. The optimal results of the proposed system demonstrate that A_{SC} is 18,900$ USD and a LCOE is 0.1478 (USD$/kWh).

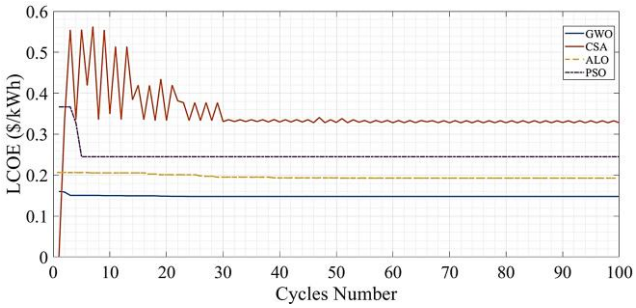

Figure 12. Comparison of LCOE among four optimization techniques (GWO, ALO, PSO, and CSA)

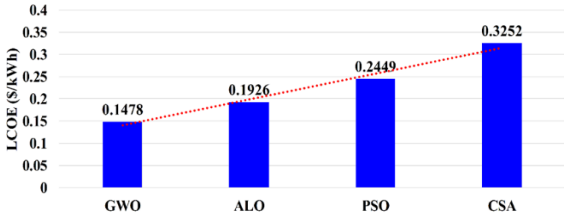

Figure 13. The comparison among four algorithms related to the levelized cost of energy

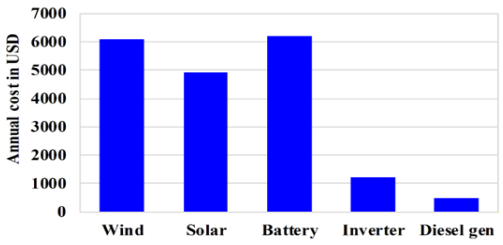

Figure 14. Annualized system cost of the proposed microgrid

Table 13. The findings of optimization techniques for the proposed system

Parameters	GWO	ALO	PSO	CSA
LCOE ($/kWh)	0.1478	0.1926	0.2449	0.3252
No. of PV (photovoltaic modules)	46	22	46	46
No. of WT (wind turbines)	30	20	10	24
No. of BATT (batteries)	10	10	10	36

10. OPTIMIZATION ALGORITHM BENCHMARKS

The current study employed GWO to obtain the optimum levelized cost of energy. It benchmarked with three other techniques: ALO, CSA, and PSO. The aim of using optimization methods is to accurately determine the optimal number of system components, maximize energy gain, and reduce energy costs by emulating some animal or insect strategies in prey acquisition. These metaheuristic techniques use equations

of costs (14-20) to obtain the optimum results. The outcome fluctuates based on the technique's context and the intricate characteristics of the data handled. The optimal LCOE obtained from the GWO technique. The finding of the proposed algorithm (GWO) is benchmarked with the results produced by the ALO, PSO, and CSA methods, respectively. The aforementioned comparison indicates that the LCOE generated by GWO outperforms its counterparts (ALO, PSO, and CSA) due to many parameters, such as the convergence speed, exploitation, and exploration.

The slower convergence speed in ALO could delay the achievement of optimum solutions, while it is faster and more stable in GWO. The convergence speed in PSO is often premature to local optima, which limits the exploration. Conversely, the GWO achieves a superior equilibrium between exploration and exploitation via its hierarchical leadership, resulting in expedited and more precise convergence. The CSA has reduced convergence speed owing to its dependence on Lévy flight-based random walks, perhaps resulting in poor exploitation of the search space. Conversely, the GWO utilizes a systematic leadership hierarchy that promotes a more equitable exploration–exploitation balance, resulting in expedited convergence to optimum solutions; hence, for all the aforementioned reasons, GWO has the first rank in reducing the LCOE [55]-[61]. Table 14 depicts the technical justification for choosing GWO in the current study.

Table 14. Technical justification for choosing GWO in the proposed microgrid [62]-[66]

Criterion	GWO	ALO	PSO	CSA
Search mechanism	Hierarchical leadership and cooperative hunting guided by α, β, and δ wolves	Random walk guided by antlion traps	Velocity–position update using global and personal best	Lévy flight-based random exploration
Exploration-exploitation balance	Well-balanced between Exploration and exploitation	Strong exploration, weaker exploitation	Fast exploitation, limited exploration	Strong exploration, limited exploitation
Nonlinear and multimodal problem handling	Highly effective	Effective	Moderately effective	Effective
Discrete decision variable suitability	High (improved solution stability)	Moderate	Moderate	Moderate
Number of control parameters	Requires few control parameters (mainly population size and iterations)	Requires moderate parameter dependency (random walk, trap parameters)	Requires moderate to high control parameters (inertia weight, cognitive and social coefficients)	Moderate (discovery probability and Lévy parameters)
Suitability for hybrid microgrid optimization	Highly suitable for mixed-integer, nonlinear techno-economic problems	Suitable	Suitable	Suitable
Convergence behavior	- Fast convergence behavior - Smooth and stable behavior	- Slow convergence during the first iterations - Possible oscillation behavior	Premature convergence	Irregular convergence behavior
Computational time	Moderate	High	Low	Moderate to high
Stability of Solutions	High solution stability and reliable outcomes throughout several iterations	Moderate stability	Low stability	Moderate stability
Statistical Performance Indicators	- Statistical Performance is stable and reliable - Consistently - Small standard deviation	- Statistical performance is unstable, less reliable, and unpredictable. - Not consistently - Larger standard deviation	Statistical performance is unreliable and unpredictable behavior - Not consistently - Big standard deviation	less predictable, poor stability, and less reliable - Low consistency - Larger standard deviation

11. CONCLUSION

As the world is focusing more on energy scavenging, renewable energy is the main focal point for today's energy policy makers and investors. However, the uncertain characteristics attributed to the resources involved motivate a diverse search for economic deployment and utilization of the resources. Hence, existing works concentrate on the development of various optimization methods to achieve sets of techno-economic objectives. This paper utilizes a GWO algorithm to implement an optimal design and optimization of a microgrid configured using PV, WT, battery bank, and Dgen support. Mathematical equations, weather resources, components' cost and specification data were deployed to aid the optimal selection of the system components. The proposed system is configured to integrate with the utility grid to meet the stochastic renewable resources and customer demands. The target customers are residential setups typically found in the

suburbs of the Baghdad metropolitan area. Objectives of the design were the optimal configurations of the microgrid for energy cost reduction and supply reliability enhancement for the customers domiciled within the case study location. Results obtained indicate an improved performance of the proposed GWO algorithm over the benchmarks of the ALO, the PSO, and the CSA algorithms by 30.3% (0.0448 $/kWh), 65.6% (0.0971 $/kWh), and 120% (0.1774 $/kWh), respectively, in terms of levelized cost of energy reduction. The suggested algorithm selects the optimum number of the proposed system, which is 46 PV modules, 30 wind turbines, and 10 units of batteries. Performance of the proposed method can be enhanced by hybridizing the algorithm with a numerical type of algorithm, such that the search space of the GWO can be fully exploited for global outcomes. Future work will enhance the suggested framework by addressing uncertainty in renewable generation and load demand utilizing stochastic approaches. Furthermore, the RB-EMS can be improved through the incorporation of adaptive or intelligent control methods, such as fuzzy logic or reinforcement learning. The optimization technique may be augmented to incorporate environmental targets, such as pollution reduction, and dynamic power pricing mechanisms to further improve both environmental and economic performance.

FUNDING INFORMATION

This work was funded by the Ministry of Higher Education under the Fundamental Research Grant Scheme (FRGS/1/2023/TK08/UTM/02/43).

AUTHOR CONTRIBUTIONS STATEMENT

This journal uses the Contributor Roles Taxonomy (CRediT) to recognize individual author contributions, reduce authorship disputes, and facilitate collaboration.

Name of Author	C	M	So	Va	Fo	I	R	D	O	E	Vi	Su	P	Fu
Sarmid Shakir Abdulsattar	✓	✓	✓	✓	✓	✓	✓	✓	✓	✓	✓		✓	
Chee Wei Tan		✓			✓	✓		✓		✓		✓		
Shahrin Ayob	✓						✓			✓		✓		✓
Yasir Shakir Abdulsattar		✓		✓	✓				✓	✓	✓			
Ahmed Tijjani Dahiru					✓					✓				✓
Chin Kim Gan		✓								✓			✓	
Kwan Yiew Lau	✓		✓				✓			✓				

C : **C**onceptualization
M : **M**ethodology
So : **So**ftware
Va : **Va**lidation
Fo : **Fo**rmal analysis
I : **I**nvestigation
R : **R**esources
D : **D**ata Curation
O : Writing - **O**riginal Draft
E : Writing - Review & **E**diting
Vi : **Vi**sualization
Su : **Su**pervision
P : **P**roject administration
Fu : **Fu**nding acquisition

CONFLICT OF INTEREST STATEMENT

The authors declare that they have no known competing financial interests or personal relationships that could have appeared to influence the work reported in this paper.

DATA AVAILABILITY

The data supporting the findings of this study are subject to confidentiality restrictions and therefore cannot be shared publicly. Additional methodological details are available from the corresponding author upon reasonable request.

REFERENCES

[1] M. Hoel and S. Kverndokk, "Depletion of fossil fuels and the impacts of global warming," *Resource and Energy Economics*, vol. 18, no. 2, pp. 115–136, Jun. 1996, doi: 10.1016/0928-7655(96)00005-X.

[2] W. Zhang, A. Maleki, and M. A. Rosen, "A heuristic-based approach for optimizing a small independent solar and wind hybrid power scheme incorporating load forecasting," *Journal of Cleaner Production*, vol. 241, p. 117920, Dec. 2019, doi: 10.1016/j.jclepro.2019.117920.

[3] S. Ahmadi and S. Abdi, "Application of the hybrid big bang–big crunch algorithm for optimal sizing of a stand-alone hybrid PV/wind/battery system," *Solar Energy*, vol. 134, pp. 366–374, Sep. 2016, doi: 10.1016/j.solener.2016.05.019.

[4] N. Bashir and B. Modu, "Techno-economic analysis of off-grid renewable energy systems for rural electrification in Northeastern Nigeria," *International Journal of Renewable Energy Research*, vol. 8, no. 3, pp. 1217–1228, 2018, doi: 10.20508/ijrer.v8i3.7126.g7422.
[5] B. Modu, M. P. Abdullah, A. L. Bukar, and M. Mustapha, "Supervisory control of solar-wind-biomass-fuel cell energy system for optimal performance," *ELEKTRIKA- Journal of Electrical Engineering*, vol. 22, no. 2, pp. 22–29, Aug. 2023, doi: 10.11113/elektrika.v22n2.463.
[6] A. Alsharif, C. W. Tan, R. Ayop, K. Y. Lau, and A. M. Dobi, "A rule-based power management strategy for vehicle-to-grid system using antlion sizing optimization," *Journal of Energy Storage*, vol. 41, p. 102913, Sep. 2021, doi: 10.1016/j.est.2021.102913.
[7] M. Bilal, P. N. Bokoro, and G. Sharma, "Hybrid optimization for sustainable design and sizing of standalone microgrids integrating renewable energy, diesel generators, and battery storage with environmental considerations," *Results in Engineering*, vol. 25, 2025, doi: 10.1016/j.rineng.2024.103764.
[8] B. Adda, M. Bouziane, A. Tayeb, H. Benbouenni, and Z. Sarra, "Enhancing photovoltaic system performance through a multi-level boost-based neural network optimization," *Studies in Science of Science*, vol. 43, no. 4, pp. 54–79, 2025.
[9] F. S. Mahmoud *et al.*, "Optimal sizing of smart hybrid renewable energy system using different optimization algorithms," *Energy Reports*, vol. 8, pp. 4935–4956, Nov. 2022, doi: 10.1016/j.egyr.2022.03.197.
[10] Y. Xu and J. Zhao, "Performance optimization of solar-wind integrated energy system with hybrid energy storage," *Solar Energy*, vol. 300, 2025, doi: 10.1016/j.solener.2025.113794.
[11] S. Yadav, P. Kumar, and A. Kumar, "Grey wolf optimization based optimal isolated microgrid with battery and pumped hydro as double storage to limit excess energy," *Journal of Energy Storage*, vol. 74, p. 109440, Dec. 2023, doi: 10.1016/j.est.2023.109440.
[12] S. Heroual, B. Belabbas, T. Allaoui, and M. Denai, "Performance enhancement of a hybrid energy storage systems using meta-heuristic optimization algorithms: genetic algorithms, ant colony optimization, and grey wolf optimization," *Journal of Energy Storage*, vol. 103, p. 114451, Dec. 2024, doi: 10.1016/j.est.2024.114451.
[13] E. Can, "DC–DC converter with multiple inputs and full isolated multi ports charging battery in photovoltaic energy systems," *Sadhana - Academy Proceedings in Engineering Sciences*, vol. 49, no. 2, 2024, doi: 10.1007/s12046-024-02506-y.
[14] S. Wang, X. Guan, and S. Liu, "Cost-effective hybrid renewable energy strategies for rural electrification: optimization-based evaluation of grid-connected and Islanded microgrid systems," *Renewable Energy*, vol. 249, p. 123274, Aug. 2025, doi: 10.1016/j.renene.2025.123274.
[15] T. O. Araoye, S. V. Egoigwe, M. J. Mbunwe, and O. A. Ezeama, "Walrus optimizer algorithm for techno-economic modeling of an autonomous hybrid microgrid energy management system," *Energy Conversion and Management*, vol. 344, p. 120277, Nov. 2025, doi: 10.1016/j.enconman.2025.120277.
[16] A. A. Rathod and B. Subramanian, "Design and optimization of various hybrid renewable energy systems using advanced algorithms for powering rural areas," *Journal of Cleaner Production*, vol. 501, p. 145199, Apr. 2025, doi: 10.1016/j.jclepro.2025.145199.
[17] A. K. Mishaal, A. M. Abd Ali, and A. B. Khamees, "Wind Distribution Map of Iraq - a comparative study," *IOP Conference Series: Materials Science and Engineering*, vol. 928, no. 2, p. 022044, Nov. 2020, doi: 10.1088/1757-899X/928/2/022044.
[18] C. Thirmal and Y. Dahman, "Different physical and chemical pretreatments of wheat straw for enhanced biobutanol production in simultaneous saccharification and fermentation," *International Journal of Energy and Environment*, vol. 2, no. 4, pp. 615–626, 2011.
[19] M. F. Zia, E. Elbouchikhi, and M. Benbouzid, "Microgrids energy management systems: a critical review on methods, solutions, and prospects," *Applied Energy*, vol. 222, pp. 1033–1055, Jul. 2018, doi: 10.1016/j.apenergy.2018.04.103.
[20] T. U. Solanke, P. K. Khatua, V. K. Ramachandaramurthy, J. Y. Yong, and K. M. Tan, "Control and management of a multilevel electric vehicles infrastructure integrated with distributed resources: a comprehensive review," *Renewable and Sustainable Energy Reviews*, vol. 144, p. 111020, Jul. 2021, doi: 10.1016/j.rser.2021.111020.
[21] C. Gamarra and J. M. Guerrero, "Computational optimization techniques applied to microgrids planning: a review," *Renewable and Sustainable Energy Reviews*, vol. 48, pp. 413–424, Aug. 2015, doi: 10.1016/j.rser.2015.04.025.
[22] E. Taymur, R. O. Bawazir, and N. Cetin, "Designing of an on-grid and off-grid PV system with battery," in *2020 2nd International Conference on Photovoltaic Science and Technologies (PVCon)*, Nov. 2020, pp. 1–6, doi: 10.1109/PVCon51547.2020.9757789.
[23] T. E. K. Zidane, S. M. Zali, M. R. Adzman, M. F. N. Tajuddin, and A. Durusu, "PV array and inverter optimum sizing for grid-connected photovoltaic power plants using optimization design," *Journal of Physics: Conference Series*, vol. 1878, no. 1, p. 012015, May 2021, doi: 10.1088/1742-6596/1878/1/012015.
[24] A. L. Bukar, C. W. Tan, and K. Y. Lau, "Optimal sizing of an autonomous photovoltaic/wind/battery/diesel generator microgrid using grasshopper optimization algorithm," *Solar Energy*, vol. 188, pp. 685–696, Aug. 2019, doi: 10.1016/j.solener.2019.06.050.
[25] A. Maleki and F. Pourfayaz, "Optimal sizing of autonomous hybrid photovoltaic/wind/battery power system with LPSP technology by using evolutionary algorithms," *Solar Energy*, vol. 115, pp. 471–483, May 2015, doi: 10.1016/j.solener.2015.03.004.
[26] S. Singh, P. Chauhan, and N. J. Singh, "Feasibility of grid-connected solar-wind hybrid system with electric vehicle charging station," *Journal of Modern Power Systems and Clean Energy*, vol. 9, no. 2, pp. 295–306, 2021, doi: 10.35833/MPCE.2019.000081.
[27] M. Bilal, I. Alsaidan, M. Alaraj, F. M. Almasoudi, and M. Rizwan, "Techno-economic and environmental analysis of grid-connected electric vehicle charging station using AI-based algorithm," *Mathematics*, vol. 10, no. 6, p. 924, Mar. 2022, doi: 10.3390/math10060924.
[28] A. F. Güven, N. Yörükeren, E. Tag-Eldin, and M. M. Samy, "Multi-objective optimization of an islanded green energy system utilizing sophisticated hybrid metaheuristic approach," *IEEE Access*, vol. 11, pp. 103044–103068, 2023, doi: 10.1109/ACCESS.2023.3296589.
[29] "Vertex 510W+ TSM-DE18M(II)," Trina Solar. [Online]. Available: https://pages.trinasolar.com/DE18M.html (accessed May 15, 2024).
[30] C. A. W. Ngouleu, Y. W. Koholé, F. C. V. Fohagui, and G. Tchuen, "Techno-economic analysis and optimal sizing of a battery-based and hydrogen-based standalone photovoltaic/wind hybrid system for rural electrification in Cameroon based on meta-heuristic techniques," *Energy Conversion and Management*, vol. 280, p. 116794, Mar. 2023, doi: 10.1016/j.enconman.2023.116794.
[31] E. Can, "A new full insulated multi output DC-DC converter for photovoltaic energy regulation and multi-battery charging," *International Journal of Electronics*, vol. 113, no. 5, pp. 891–913, May 2026, doi: 10.1080/00207217.2025.2562994.

[32] A. L. Bukar, C. W. Tan, L. K. Yiew, R. Ayop, and W.-S. Tan, "A rule-based energy management scheme for long-term optimal capacity planning of grid-independent microgrid optimized by multi-objective grasshopper optimization algorithm," *Energy Conversion and Management*, vol. 221, p. 113161, Oct. 2020, doi: 10.1016/j.enconman.2020.113161.
[33] R. Shi, S. Li, P. Zhang, and K. Y. Lee, "Integration of renewable energy sources and electric vehicles in V2G network with adjustable robust optimization," *Renewable Energy*, vol. 153, pp. 1067–1080, Jun. 2020, doi: 10.1016/j.renene.2020.02.027.
[34] M. A. M. Ramli, H. R. E. H. Bouchekara, and A. S. Alghamdi, "Optimal sizing of PV/wind/diesel hybrid microgrid system using multi-objective self-adaptive differential evolution algorithm," *Renewable Energy*, vol. 121, pp. 400–411, Jun. 2018, doi: 10.1016/j.renene.2018.01.058.
[35] Inverter.com, "1000W Horizontal Axis Wind Turbine, 24V/48V," *Inverter.Com*. https://www.inverter.com/1000w-wind-turbine (accessed May 15, 2024).
[36] F. A. T. Konchou, H. D. Temene, R. Tchinda, and D. Njomo, "Techno-economic and environmental design of an optimal hybrid energy system for a community multimedia centre in Cameroon," *SN Applied Sciences*, vol. 3, no. 1, p. 127, Jan. 2021, doi: 10.1007/s42452-021-04151-0.
[37] R. Dufo-López *et al.*, "Multi-objective optimization minimizing cost and life cycle emissions of stand-alone PV–wind–diesel systems with batteries storage," *Applied Energy*, vol. 88, no. 11, pp. 4033–4041, Nov. 2011, doi: 10.1016/j.apenergy.2011.04.019.
[38] A. Yahiaoui, F. Fodhil, K. Benmansour, M. Tadjine, and N. Cheggaga, "Grey wolf optimizer for optimal design of hybrid renewable energy system PV-diesel generator-battery: application to the case of Djanet city of Algeria," *Solar Energy*, vol. 158, pp. 941–951, Dec. 2017, doi: 10.1016/j.solener.2017.10.040.
[39] M. H. Amrollahi and S. M. T. Bathaee, "Techno-economic optimization of hybrid photovoltaic/wind generation together with energy storage system in a stand-alone micro-grid subjected to demand response," *Applied Energy*, vol. 202, pp. 66–77, Sep. 2017, doi: 10.1016/j.apenergy.2017.05.116.
[40] S. Singh, M. Singh, and S. C. Kaushik, "Feasibility study of an islanded microgrid in rural area consisting of PV, wind, biomass and battery energy storage system," *Energy Conversion and Management*, vol. 128, pp. 178–190, Nov. 2016, doi: 10.1016/j.enconman.2016.09.046.
[42] S. Barakat, H. Ibrahim, and A. A. Elbaset, "Multi-objective optimization of grid-connected PV-wind hybrid system considering reliability, cost, and environmental aspects," *Sustainable Cities and Society*, vol. 60, p. 102178, Sep. 2020, doi: 10.1016/j.scs.2020.102178.
[41] A. Elbaz and M. T. Guneser, "Multi-objective optimization method for proper configuration of grid-connected PV-wind hybrid system in terms of ecological effects, outlay, and reliability," *Journal of Electrical Engineering & Technology*, vol. 16, no. 2, pp. 771–782, Mar. 2021, doi: 10.1007/s42835-020-00635-y.
[43] S. N. Motapon, L.-A. Dessaint, and K. Al-Haddad, "A comparative study of energy management schemes for a fuel-cell hybrid emergency power system of more-electric aircraft," *IEEE Transactions on Industrial Electronics*, vol. 61, no. 3, pp. 1320–1334, Mar. 2014, doi: 10.1109/TIE.2013.2257152.
[44] X. Zhao *et al.*, "Energy management strategies for fuel cell hybrid electric vehicles: classification, comparison, and outlook," *Energy Conversion and Management*, vol. 270, p. 116179, Oct. 2022, doi: 10.1016/j.enconman.2022.116179.
[45] L. Olatomiwa, S. Mekhilef, M. S. Ismail, and M. Moghavvemi, "Energy management strategies in hybrid renewable energy systems: a review," *Renewable and Sustainable Energy Reviews*, vol. 62, pp. 821–835, Sep. 2016, doi: 10.1016/j.rser.2016.05.040.
[46] A. R. Bhatti and Z. Salam, "A rule-based energy management scheme for uninterrupted electric vehicles charging at constant price using photovoltaic-grid system," *Renewable Energy*, vol. 125, pp. 384–400, Sep. 2018, doi: 10.1016/j.renene.2018.02.126.
[47] X. Jiang and C. Xiao, "Household energy demand management strategy based on operating power by genetic algorithm," *IEEE Access*, vol. 7, pp. 96414–96423, 2019, doi: 10.1109/ACCESS.2019.2928374.
[48] X. Ji, Q. Liu, Z. Liu, Y. Xie, and J. Zhai, "Coordinated control and power management of diesel-PV-battery in hybrid stand-alone microgrid system," *The Journal of Engineering*, vol. 2019, no. 18, pp. 5245–5249, Jul. 2019, doi: 10.1049/joe.2018.9290.
[49] S. B. Darling, F. You, T. Veselka, and A. Velosa, "Assumptions and the levelized cost of energy for photovoltaics," *Energy & Environmental Science*, vol. 4, no. 9, p. 3133, 2011, doi: 10.1039/c0ee00698j.
[50] B. Modu, M. P. Abdullah, A. Alkassem, and M. F. Hamza, "Optimal rule-based energy management and sizing of a grid-connected renewable energy microgrid with hybrid storage using Levy flight algorithm," *Energy Nexus*, vol. 16, p. 100333, Dec. 2024, doi: 10.1016/j.nexus.2024.100333.
[51] A. H. Fathima and K. Palanisamy, "Optimization in microgrids with hybrid energy systems – a review," *Renewable and Sustainable Energy Reviews*, vol. 45, pp. 431–446, May 2015, doi: 10.1016/j.rser.2015.01.059.
[52] A. S. Assiri, A. G. Hussien, and M. Amin, "Ant lion optimization: variants, hybrids, and applications," *IEEE Access*, vol. 8, pp. 77746–77764, 2020, doi: 10.1109/ACCESS.2020.2990338.
[53] M. Thirunavukkarasu, Y. Sawle, and H. Lala, "A comprehensive review on optimization of hybrid renewable energy systems using various optimization techniques," *Renewable and Sustainable Energy Reviews*, vol. 176, p. 113192, Apr. 2023, doi: 10.1016/j.rser.2023.113192.
[54] P. Sharma, A. Saxena, B. P. Soni, R. Kumar, and V. Gupta, "An intelligent energy bidding strategy based on opposition theory enabled grey wolf optimizer," in *2018 International Conference on Power, Instrumentation, Control and Computing (PICC)*, Jan. 2018, pp. 1–6, doi: 10.1109/PICC.2018.8384802.
[55] A. Tabak, E. Kayabasi, M. T. Guneser, and M. Ozkaymak, "Grey wolf optimization for optimum sizing and controlling of a PV/WT/BM hybrid energy system considering TNPC, LPSP, and LCOE concepts," *Energy Sources, Part A: Recovery, Utilization, and Environmental Effects*, vol. 44, no. 1, pp. 1508–1528, Mar. 2022, doi: 10.1080/15567036.2019.1668880.
[56] M. Abdulgader, S. Lakshminarayanan, and D. Kaur, "Efficient energy management for smart homes with grey wolf optimizer," in *2017 IEEE International Conference on Electro Information Technology (EIT)*, May 2017, pp. 388–393, doi: 10.1109/EIT.2017.8053392.
[57] Q. Li, Z. Cui, Y. Cai, and Y. Su, "Multi-objective operation of solar-based microgrids incorporating artificial neural network and grey wolf optimizer in digital twin," *Solar Energy*, vol. 262, p. 111873, Sep. 2023, doi: 10.1016/j.solener.2023.111873.
[58] N. M. Hatta, A. M. Zain, R. Sallehuddin, Z. Shayfull, and Y. Yusoff, "Recent studies on optimisation method of grey wolf optimiser (GWO): a review (2014–2017)," *Artificial Intelligence Review*, vol. 52, no. 4, pp. 2651–2683, Dec. 2019, doi: 10.1007/s10462-018-9634-2.
[59] M. Mareli and B. Twala, "An adaptive Cuckoo search algorithm for optimisation," *Applied Computing and Informatics*, vol. 14, no. 2, pp. 107–115, 2018, doi: 10.1016/j.aci.2017.09.001.
[60] D. Wang, D. Tan, and L. Liu, "Particle swarm optimization algorithm: an overview," *Soft Computing*, vol. 22, no. 2, pp. 387–408, Jan. 2018, doi: 10.1007/s00500-016-2474-6.

[61] H. Kilic, U. Yuzgec, and C. Karakuzu, "A novel improved antlion optimizer algorithm and its comparative performance," *Neural Computing and Applications*, vol. 32, no. 8, pp. 3803–3824, Apr. 2020, doi: 10.1007/s00521-018-3871-9.
[62] S. Mirjalili, S. M. Mirjalili, and A. Lewis, "Grey wolf optimizer," *Advances in Engineering Software*, vol. 69, pp. 46–61, Mar. 2014, doi: 10.1016/j.advengsoft.2013.12.007.
[63] Q. Bai, "Analysis of particle swarm optimization algorithm," *Computer and Information Science*, vol. 3, no. 1, pp. 180–184, Jan. 2010, doi: 10.5539/cis.v3n1p180.
[64] J. E. Bell and P. R. McMullen, "Ant colony optimization techniques for the vehicle routing problem," *Advanced Engineering Informatics*, vol. 18, no. 1, pp. 41–48, Jan. 2004, doi: 10.1016/j.aei.2004.07.001.
[65] S. Mirjalili, A. Lewis, and A. S. Sadiq, "Autonomous particles groups for particle swarm optimization," *Arabian Journal for Science and Engineering*, vol. 39, no. 6, pp. 4683–4697, Jun. 2014, doi: 10.1007/s13369-014-1156-x.
[66] M. Imran, R. Hashim, and N. E. A. Khalid, "An overview of particle swarm optimization variants," *Procedia Engineering*, vol. 53, pp. 491–496, 2013, doi: 10.1016/j.proeng.2013.02.063.

APPENDIX

Table 1. Critical analysis/limitations of the previous studies

Author(s)	Year	System configuration	Grid connection	Optimization technique	Objectives	Key finding	Limitations
Mahmoud *et al.* [9]	2022	- PV system - Wind turbine - Battery storage bank - Diesel generator	Off-grid	- Grey wolf optimization (GWO) - Improved grey wolf optimization (IGWO) - Salp swarm algorithm (SSA)	- Reduce energy cost (COE) - Minimize loss of power supply probability (LPSP)	IGWO achieved - Lower COE (≈ 0.21582 $/kWh) - Increase the speed of convergence	- Did not consider grid integration - Did not use dynamic electricity pricing
Xu and Zhao [10]	2025	- Solar thermal system - Wind turbines - Thermal storage unit - Hydrogen storage unit	Grid-connected	- Grey wolf optimizer (GWO) - Multi-objective grey wolf optimizer (MOGWO)	- Maximize net present value (NPV) - Increase the efficiency of renewable utilization - Reduce CO_2 emissions	- GWO produced the greatest economic advantage (NPV ≈ 122.6 M$). - GWO reaches around 29.7% renewable efficiency.	- Installation system cost is ignored
Yadav *et al.* [11]	2023	- PV system - Battery storage bank - Inverter - Wind turbine - Hydro storage pump	Standalone (isolated microgrid)	- Grey wolf optimizer (GWO) - Moth flame optimization (MFO) - Dragonfly algorithm (DA)	- Reduce levelized cost of energy (LCOE) - Attaining a 100% renewable percentage	- GWO reduces the LCOE to (0.3588 $/kWh) - GWO demonstrates faster convergence	- Did not consider grid integration - Real-time control is not considered.
Heroual *et al.* [12]	2024	- PV system - Hybrid storage system (battery and supercapacitor) - Converter	Off-grid	- Grey wolf optimizer (GWO) - Genetic algorithm (GA) - Ant colony optimization (ACO)	- Improve energy management system performance - Decrease battery stress	- GWO provides the fastest settling time - GWO outperforms ACO and GA	- Levelized cost of energy (LCOE) is not considered - Did not consider grid integration
Can *et al.* [13]	2024	- PV system - Battery storage bank - DC-DC converter	Standalone	Converter topology design	- Increase power efficiency - Increases battery life using adaptable charging methods	Stable output voltage, multiple modes of battery charging capabilities, and reduce no. of components are all confirmed by simulation and experimental findings.	- Not consider stochastic renewable variability - Did not consider grid integration

Table 1. Critical analysis/limitations of the previous studies (continued)

Author(s)	Year	System configuration	Grid connection	Optimization technique	Objectives	Key finding	Limitations
Wang *et al.* [14]	2025	- PV system - Battery storage bank - Wind turbine - Converter - Biomass plant	- Grid-connected - Off-grid	- Seagull optimization algorithm (SOA) - Tree physiology optimization (TPO) - Invasive weed optimization (IWO) - Biogeography-based optimization (BBO)	- Minimize net present cost (NPC) - Decrease levelized cost of energy (LCOE)	SOA achieved the lowest costs In case of - On-grid LCOE = 0.076 $/kWh and NPC = 1,355,437 $ - Off-grid LCOE = 0.139 $/kWh and NPC = 1,821,323 $ (off-grid)	Did not consider the real-time energy management control scheme
Araoye *et al.* [15]	2025	- PV system, - Wind turbine - Hydropower - Biogas system - Diesel generator -Battery storage bank - Power converter	Autonomous	- Walrus optimizer (WO) - Grey wolf optimization (GWO) - Particle swarm optimization (PSO)	- Reduce cost of energy (COE) - Minimize net present cost (NPC) - Reducing emissions	WO achieved - Faster convergence - Low COE (0.005081 $/kWh) - 0% emissions - Reduce NPC	- Energy management strategies are not addressed - Did not consider grid integration
Rathod and Subramanian [16]	2025	- PV system - Wind turbine - Battery storage bank	Grid-connected	- Grey wolf–whale optimization algorithm (EGW–WOA) - Whale optimization algorithm - Genetic algorithm (GA) - Grey wolf optimization (GWO)	- Reduce system cost	EGW–WOA - Decrease 24-h operating cost by 18.6% - Attained the lowest average cost (≈ $293,859)	- Did not consider the long-term operational scheduling - Did not calculate the component size
This study		- PV system - Wind turbine - Diesel generator - Storage battery bank	Grid-connected	- Grey wolf optimization (GWO) - Particle swarm optimization (PSO) - Cuckoo search algorithm (CSA) - Ant lion algorithm (ALO)	- Minimize levelized cost of energy (LCOE) - Optimal system components	GWO achieved - Minimum LCOE with realistic EMS - Selecting optimum system components - Export the excess energy to the grid	Does not consider the CO2 emission

BIOGRAPHIES OF AUTHORS

Sarmid Shakir Abdulsattar received the B.Sc. degree in laser engineering from the University of Technology, Iraq, in 2008, and the M.Sc. degree in renewable energy and energy efficiency from Kassel University, Germany, in 2013. He is currently pursuing a Ph.D. degree in Electrical Engineering at the Universiti Teknologi Malaysia, Malaysia. He is a researcher at the Solar Energy Research Centre at the Ministry of Science and Technology, Iraq. His research interests in microgrid systems combined with energy management strategies based on the application of optimization techniques. He published several papers on renewable energy optimization techniques. He can be contacted at email: eng.sarmad86@yahoo.com.

Chee Wei Tan received his B.Eng. degree in electrical engineering (first class honors) from Universiti Teknologi Malaysia (UTM) in 2003 and a Ph.D. degree in electrical engineering from Imperial College London, London, U.K., in 2008. He is currently an associate professor at Universiti Teknologi Malaysia and a member of the Power Electronics and Drives Research Group, Faculty of Electrical Engineering, as well as an associate member with the Centre of Electrical Energy Systems (CEES). His research interests include the application of power electronics in renewable/alternative energy systems, control of power electronics, and energy management systems in microgrids. He can be contacted at email: cheewei@utm.my.

Shahrin bin Ayob is an associate professor in the field of electrical power engineering at Universiti Teknologi Malaysia (UTM). He earned his bachelor's degree in electrical engineering in 2001, followed by a master's degree in electrical engineering (power) in 2003, and a Ph.D. in 2009, all from at Universiti Teknologi Malaysia. A senior member of IEEE, his research interests span power electronics, electric vehicle technologies, fuzzy control systems, and education engineering. Over the years, he has published extensively in reputable journals and conferences, contributing significantly to advancements in sustainable energy and intelligent control systems. He can be contacted at email: shahrin@fke.utm.my.

Yasir Shakir Abdulsattar received the B.Sc. degree in mechanical engineering from the University of Technology, Baghdad, Iraq, and his M.Sc. degree in Thermal Energy from Karabuk University, Turkey (2023). He is currently working at the National Center of Engineering Consultancy. As well as making studies and research about the optimization of algorithms using MATLAB and numerical analysis software. Renewable energy, energy management systems, energy efficiency, and sustainable energy applications are a major part of his interests. He can be contacted at email: yasiralsarraj@gmail.com.

Ahmed Tijjani Dahiru is a chief lecturer at the Federal College of Education (Technical), Bichi, Kano, Nigeria. He holds an M.Sc. in electrical and electronic engineering from the University of Bradford (2013), United Kingdom, and a Ph.D. in electrical engineering from Universiti Teknologi Malaysia (2021). His research interests include renewable energy system planning, implementation, and energy management based on the application of optimization techniques. He can be contacted at email: babanbushra@gmail.com.

Chin Kim Gan received the B.Eng. and M.Eng. degrees in electrical engineering from the Universiti Teknologi Malaysia and the Ph.D. degree from Imperial College London. He is currently a professor with the Faculty of Electrical Technology and Engineering, Universiti Teknikal Malaysia Melaka. He can be contacted at email: ckgan@utem.edu.my.

Kwan Yiew Lau is an associate professor at the Institute of High Voltage and High Current, Faculty of Electrical Engineering, Universiti Teknologi Malaysia. He received his B.Eng. degree in electrical engineering (first class honors) and M.Eng. degree in electrical power engineering from Universiti Teknologi Malaysia in 2007 and 2010, respectively, and his Ph.D. degree in electronics and electrical engineering from the University of Southampton, UK, in 2013. His research interests include high voltage engineering, dielectric materials, and renewable energy systems. He can be contacted at email: kwanyiew@utm.my.